

# Simultaneous Acquisition of the Polarized and Depolarized Raman Signal with a Single Detector

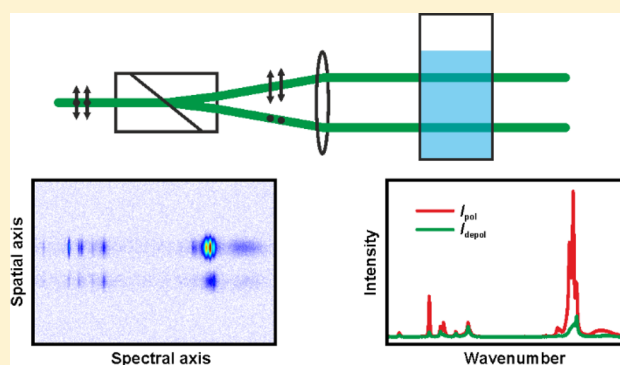
Johannes Kiefer<sup>\*,†,‡,§</sup>

<sup>†</sup>Technische Thermodynamik and MAPEX Center for Materials and Processes, Universität Bremen, Badgasteiner Strasse 1, 28359 Bremen, Germany

<sup>‡</sup>School of Engineering, University of Aberdeen, Aberdeen AB24 3UE, United Kingdom

<sup>§</sup>Erlangen Graduate School in Advanced Optical Technologies (SAOT), Friedrich-Alexander-Universität Erlangen-Nürnberg, Erlangen, Germany

**ABSTRACT:** Polarization-resolved Raman spectroscopy provides much more information than its conventional counterpart. However, it usually either requires a complicated setup with two spectrographs and detectors or two measurements must be performed sequentially. This study presents a simple and straightforward approach to recording both polarization components simultaneously with a single spectrograph and detector. The vertically and a horizontally polarized laser beam exiting a Wollaston prism are focused into the sample with a small spatial separation. The scattered light from both beams is imaged onto the slit of an imaging spectrograph as two spatially separated signals, i.e., the polarized and the depolarized Raman signal. Eventually, both spectra are acquired on a single CCD chip simultaneously. Experimental data of ethanol and dimethyl sulfoxide are shown as proof-of-concept. The new method has a number of advantages, for example, laser intensity fluctuations and the polarization dependence of the diffraction grating do not play a role. The proposed approach will be useful for an improved structural analysis and it will be the enabling technology for temporally resolved enantioselective Raman (esR) spectroscopy.



With the invention of the laser in 1960, Raman spectroscopy became a versatile tool for qualitative and quantitative chemical analysis. Nowadays, it is a well-established method in analytical laboratories and in the field. Common applications include combustion diagnostics,<sup>1,2</sup> process monitoring,<sup>3,4</sup> structural analysis,<sup>5,6</sup> the investigation of molecular interactions,<sup>7,8</sup> as well as label-free microscopy with chemical contrast in biomedicine and material science.<sup>9,10</sup>

A key feature of Raman scattering is its sensitivity to the polarization properties of the incident light. If the laser is linearly polarized, the majority of the Raman signal will be polarized in the same way. This is due to the virtually instantaneous scattering event during which the polarization state is maintained. A small fraction of the scattered light, however, will be polarized orthogonally with respect to the incident light. This is referred to as the depolarized signal. The ratio of the depolarized and polarized signal components is the depolarization ratio  $\rho$ .<sup>11–13</sup> Its value allows deriving valuable information about the symmetry of a vibrational mode, for instance.<sup>14,15</sup> Consequently, acquiring both the polarized and the depolarized Raman spectrum permits an improved structural analysis, a more accurate assignment of peaks, and possibly gaining a multitude of additional information. Moreover, polarization-resolved detection enables the determi-

nation of the isotropic and anisotropic Raman intensities,  $I_{\text{iso}}$  and  $I_{\text{aniso}}$  via

$$I_{\text{iso}} = I_{\text{VV}} - \frac{4}{3}I_{\text{VH}} \quad (1)$$

$$I_{\text{aniso}} = I_{\text{VH}} \quad (2)$$

where  $I_{\text{VV}}$  and  $I_{\text{VH}}$  are the vertically and horizontally polarized signal components, respectively.<sup>15,16</sup> The indices VV and VH indicate that the incident laser is in both cases vertically polarized (first character) and the vertically and horizontally polarized signal components are detected separately (second character). Further advantages of polarization-resolved Raman spectroscopy include the suppression of fluorescence interferences in combustion diagnostics<sup>17</sup> and the possibility of discriminating enantiomers in chiral media.<sup>18,19</sup>

There are several common approaches of performing polarization-resolved Raman spectroscopy experiments. The simplest one employs a polarization filter, either a thin film polarizer or a polarizing prism, in the signal collection path, e.g., between a collimating and a focusing lens. To obtain the

**Received:** March 25, 2017

**Accepted:** May 9, 2017

**Published:** May 9, 2017

vertical or the horizontal signal component, the polarizer is oriented accordingly. Despite its simplicity, this approach has two disadvantages: first, the two spectra must be recorded sequentially and, as a consequence, it does not permit temporally resolved measurements; second, a polarization scrambler is required to compensate for the polarization-dependent efficiency of the optical components in the spectrograph.<sup>11</sup> Such a scrambler may also reduce the signal intensity and hence it calls for longer acquisition times. Another option to avoid polarization-dependent effects in the spectrograph is to flip the polarization direction of the laser using a half-wave plate.<sup>11,20</sup> Again, the two spectra must be recorded in sequence. Nevertheless, acquiring both the polarized and depolarized signal components simultaneously is possible using a polarizing beam splitter in the signal path and two spectrometers.<sup>3,17</sup> This approach, however, is inherently expensive and requires significant alignment effort. Moreover, the detectors must be synchronized. Therefore, the simultaneous acquisition of the polarized and depolarized Raman signals with a single detector would be a substantial advancement. Furthermore, it would reduce the costs by nearly 50% compared to the common setup with two spectrographs and two cameras, as these two components are the main cost drivers in a Raman experiment.

## METHOD

Simultaneous acquisition of both signals can be achieved by utilizing and modifying the 40 years old idea of simultaneously mapping the excitation-wavelength-resolved fluorescence emission spectrum.<sup>21,22</sup> In this approach, the radiation of a broadband light source is dispersed in the measurement volume. The resulting illuminated line is then imaged onto the entrance slit of an imaging spectrograph. Consequently, the camera attached to the spectrograph records an image, in which the vertical direction represents the excitation wavelength while the horizontal axis corresponds to the emission wavelength. This elegant method was proposed by Warner et al.<sup>21,22</sup> and is currently experiencing a renaissance in fluorescence spectroscopy with supercontinuum sources<sup>23</sup> and Raman spectroscopy with light-emitting diodes<sup>24,25</sup> and commercial laser pointers.<sup>26</sup>

In the present study, the underlying concept is borrowed to achieve the simultaneous acquisition of the polarized and depolarized Raman signals with a single detector. For this purpose, instead of dispersing the radiation of a broadband light source, the vertical and horizontal components of a linearly polarized laser beam are focused into the measurement volume (e.g., in a cuvette holding the sample) at slightly different positions. This can be obtained as illustrated in Figure 1. The vertically polarized laser beam initially passes a polarizing prism to reject any unpolarized components. Then, a half-wave plate rotates the polarization plane by 45° so that the vertical and horizontally polarized projections are identical in intensity. The two components are subsequently separated from each other in a Wollaston prism,<sup>27</sup> see zoomed-in feature of Figure 1. A lens with a focal length matching the angle of the outgoing beams from the prism makes the beams parallel and focuses them into the measurement volume at the same time. The scattered light from both beams is imaged onto the entrance slit of an imaging spectrograph equipped with a sensitive charge-coupled device (CCD) detector. The image contains the polarized and depolarized Raman signal as illustrated in the upper right corner of Figure 1. Such a single-detector acquisition of two Raman signals utilizing an imaging spectrograph has also been

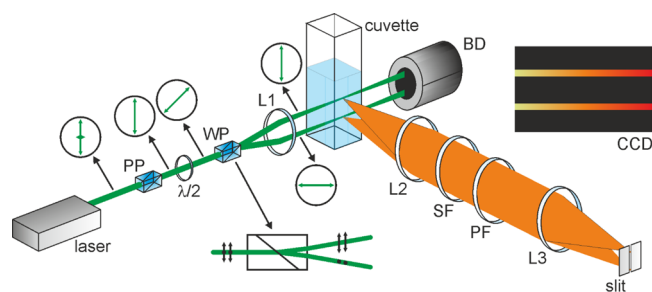


**Figure 1.** Schematic experimental setup. PP = polarizing prism;  $\lambda/2$  = half-wave plate; WP = Wollaston prism; L1–L3 = lenses; SF = spectral filter; PF = polarization filter; BD = beam dump; CCD = charge-coupled device chip.

employed for Raman difference spectroscopy. For this purpose, Frosch et al. guided the signal from two different measurement cells to the spectrograph slit using a bifurcated fiber bundle with a linear end to illuminate different parts of the slit.<sup>28</sup>

## PROOF-OF-CONCEPT

Proof-of-concept experiments were carried out using a diode-pumped solid state laser (Nd:YAG, 532 nm, 80 mW). An arrangement of a Glan-Thompson prism, a multiorder half-wave plate, a Wollaston prism, and a 200 mm focal length lens provided two parallel, one vertically, and one horizontally polarized beams. The beams had a distance of  $\sim 3.5$  mm and were focused into a cuvette holding a liquid sample. The scattered light from both beams was collected and collimated, spectrally (dielectric long-pass filter, cutoff 550 nm) and polarization filtered (broadband polarizing beam splitter cube oriented such that only vertically polarized light is transmitted toward the spectrograph), and focused onto the entrance slit of an imaging spectrograph (Princeton Instruments, Acton 2300i, 300 mm focal length, 600 grooves/mm). An intensified CCD camera (Andor, iStar, 1024  $\times$  1024 pixel) recorded the images containing both signal components. The acquisition time was 500 ms. Measurements were performed with pure ethanol and dimethyl sulfoxide. In order to obtain the full spectral range of interest from  $\sim 300$  to  $\sim 3800$   $\text{cm}^{-1}$  with high resolution, two images had to be recorded and merged for each sample. Note that the dielectric long-pass filter was angle-tuned to shift the cutoff wavelength in order to facilitate recording the Raman spectrum from 300  $\text{cm}^{-1}$ .

The merged images and the resulting polarized and depolarized Raman spectra are displayed in Figure 2. The two signal components are well separated on the CCD chip and thus they can be extracted easily. Vertically binning the areas indicated by the dashed lines in Figure 2A,B obtains spectra with a high signal-to-noise ratio and high spectral resolution. Differences in the depolarization ratio are obvious looking at individual lines. Some of them are virtually completely polarized, i.e., the depolarized spectrum is flat, while others are nearly depolarized, i.e., a depolarization ratio close to 0.75.<sup>29</sup> A detailed list of peaks of ethanol and DMSO and their assignment is given in Table 1.

The CH stretching region between 2700 and 3100  $\text{cm}^{-1}$  highlights the advantages of polarization-resolved Raman spectroscopy in the structural analysis. This part of the spectrum is particularly complicated and difficult to analyze due to the multitude of vibrational modes overlapping with each other. There are symmetric and antisymmetric CH stretching modes but also overtone and combination bands

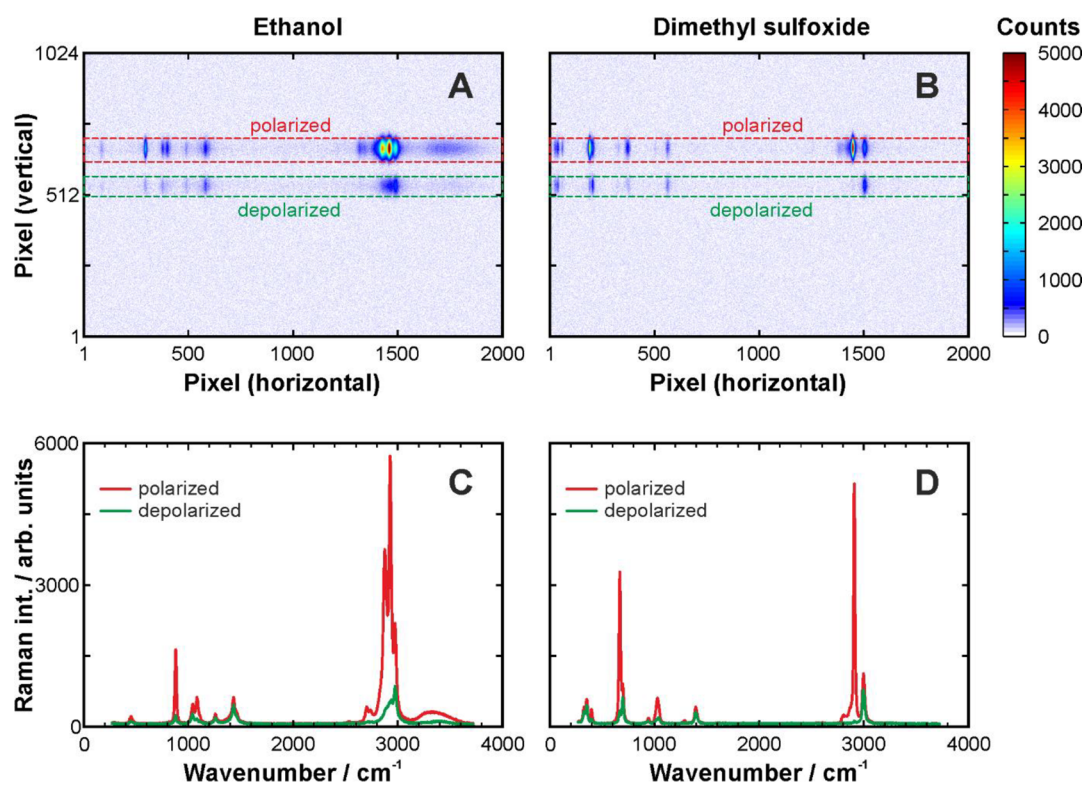


**Figure 2.** Experimental signals from ethanol (A and C) and DMSO (B and D). Panels A and B show the recorded images, and panels C and D show the derived spectra. Note that the images panels A and B were combined from two images recorded with high resolution in the ranges  $\sim 300\text{--}2000$  and  $\sim 2000\text{--}3800$   $\text{cm}^{-1}$ . Hence, the total number of  $\sim 2000$  pixels in horizontal direction.

**Table 1.** Wavenumbers and Depolarization Ratios of Observed Raman Peaks and Their Vibrational Assignment<sup>a</sup>

ethanol			dimethyl sulfoxide		
$\nu$ in $\text{cm}^{-1}$	$\rho$	assignment	$\nu$ in $\text{cm}^{-1}$	$\rho$	assignment
3323		OH str			
2974	0.38	CH <sub>3</sub> as str	2999	0.68	CH <sub>3</sub> as str
2927	0.09	CH <sub>3</sub> s str	2910	0.01	CH <sub>3</sub> s str
2876	0.08	CH <sub>2</sub> s str	2811	0	combination
2741	0.16	combination	1395	0.70	CH <sub>2</sub> sciss
2703	0.15	combination	1287	0	CH <sub>2</sub> wag
1458sh	0.73	CH <sub>2</sub> sciss	1031	0.22	SO str
1433	0.74	CH <sub>2</sub> sciss	942	0.45	CH <sub>2</sub> rock
1258	0.65	CH <sub>2</sub> wag	698	0.66	CSC as str
1083	0.22	CH <sub>3</sub> rock	670	0.09	CSC s str
1040	0.51	CC as str	400	0.32	CSO rock
879	0.13	CC s str	353	0.75	CSO bend
454	0.40	CCO bend	332	0.75	CSO bend

<sup>a</sup>sh = shoulder; str = stretching; as = anti-symmetric; s = symmetric; sciss = scissoring; rock = rocking; wag = wagging.

arising from the normal modes in the fingerprint region. The latter can be enhanced by Fermi resonance, which leads to frequency-shifts and intensity changes adding further complexity.<sup>30–33</sup> As mentioned above, the depolarization ratio depends on the symmetry of a vibration. Highly symmetric modes have a low depolarization and antisymmetric modes behave the opposite. The DMSO spectrum has two main peaks in the CH stretching region and the depolarized signal clearly shows that the one at  $2999\text{ cm}^{-1}$  corresponds to the antisymmetric mode. The spectrum of ethanol, on the other hand, is more complex due to the CH<sub>2</sub> and CH<sub>3</sub> groups. Nevertheless, even there, the

depolarized spectrum reveals dominating contributions of antisymmetric modes in the high-wavenumber part of the CH band. The depolarization ratio of these antisymmetric modes is not as high as 0.75 but still about four times the value of the corresponding symmetric modes.

To validate the new method, a comparison is made taking the antisymmetric and symmetric stretching CSC modes of DMSO at  $698$  and  $670\text{ cm}^{-1}$ , respectively, as an example. The proposed simultaneous technique delivers  $0.66$  and  $0.09$  for the depolarization ratio. The conventional approach employing two spectrometers and a polarizing beam splitter (see ref 3) yielded  $0.62$  and  $0.12$ . Furthermore, Skripkin et al.<sup>34</sup> reported  $0.75$  and  $0.11$ , while Sastry et al.<sup>35</sup> gave  $0.65$  and  $0.09$  in their work. This puts the new approach well in between the published data. However, the comparison also highlights that the measurement of the depolarization ratio is obviously subject to a certain measurement uncertainty. If two consecutive spectra must be acquired, the laser stability is crucial and even small changes can lead to significant errors. The same is true when two detectors are used, since their response function and quantum efficiency may be slightly different. In addition, there may be different losses when coupling the vertically and horizontally polarized signal components into different spectrometers. These sources of uncertainty and systematic error are automatically eliminated by the proposed method as the two spectra are recorded simultaneously with the same detector. Nevertheless, systematic errors in the new approach can evolve when the laser intensity in both legs of the beam, i.e., the vertically and horizontally polarized part after the Wollaston prism, is not identical. Hence, care must be taken in the adjustment of the half-wave plate, e.g., using a photodiode or power meter during the initial alignment.

## CONCLUSION

In conclusion, an experimental concept for the simultaneous acquisition of the polarized and depolarized Raman signal with a single detector has been proposed and demonstrated. For this purpose, two parallel beams with orthogonal polarization are focused into the sample. The scattered light from both beams is imaged onto the entrance slit of an imaging spectrograph equipped with a CCD detector. This facilitates recording both spectra simultaneously within a fraction of a second. Proof-of-concept experiments were carried out in ethanol and dimethyl sulfoxide.

Advantages of the proposed method include the following: (i) only a single spectrograph and detector is needed, (ii) laser intensity fluctuations do not introduce measurement errors, (iii) polarization-dependent effects of the diffraction grating in the spectrograph do not play a role, (iv) uncertainties due to quantum efficiency and gain differences of two-detector methods are avoided, and (v) it offers the possibility for measurements with high temporal resolution.

On the other hand, disadvantages include (i) a 2D array detector is needed, (ii) the sample must be homogeneous on the length scale of the beam separation distance, and (iii) misalignment of the half-wave plate will result in systematic errors.

The new method will not only be useful for an improved structural analysis. In our lab, it will be taken forward as enabling technology for a simplified approach to temporally resolved enantioselective Raman (esR) spectroscopy based on the method proposed and characterized recently.<sup>18,19,36</sup> The aim is to develop the esR technique as a versatile tool for process monitoring during the production of enantiopure chiral substances, e.g., pharmaceutically active ingredients.

## AUTHOR INFORMATION

### Corresponding Author

\*E-mail: [jkiefer@uni-bremen.de](mailto:jkiefer@uni-bremen.de).

### ORCID

Johannes Kiefer: 0000-0002-0837-3456

### Notes

The author declares no competing financial interest.

## ACKNOWLEDGMENTS

The author would like to thank Colin D. Bain (University of Durham, U.K.) for the fruitful discussion at the 2016 SciX–The Great Scientific eXchange, during which the idea for the proposed approach was born. Furthermore, financial support of this work from Deutsche Forschungsgemeinschaft (DFG) through Grant KI1396/4-1 is gratefully acknowledged.

## REFERENCES

- (1) Eckbreth, A. C. *Laser Diagnostics for Combustion Temperature and Species*, 2nd ed.; Gordon and Breach: Amsterdam, The Netherlands, 1996.
- (2) Ehn, A.; Zhu, J.; Li, X.; Kiefer, J. *Appl. Spectrosc.* **2017**, *71*, 341–366.
- (3) Noack, K.; Eskofier, B.; Kiefer, J.; Dilk, C.; Bilow, G.; Schirmer, M.; Buchholz, R.; Leipertz, A. *Analyst* **2013**, *138*, S639–S646.
- (4) Knopke, L. R.; Nemati, N.; Kockritz, A.; Bruckner, A.; Bentrup, U. *ChemCatChem* **2010**, *2*, 273–280.
- (5) Frosch, T.; Popp, J. *J. Mol. Struct.* **2009**, *924*, 301–308.
- (6) Christodoulakis, A.; Boghosian, S. *J. Catal.* **2008**, *260*, 178–187.
- (7) Noack, K.; Kiefer, J.; Leipertz, A. *ChemPhysChem* **2010**, *11*, 630–637.

- (8) Paschoal, V. H.; Faria, L. F. O.; Ribeiro, M. C. C. *Chem. Rev.* **2017**, DOI: 10.1021/acs.chemrev.6b00461.
- (9) Everall, N. *Appl. Spectrosc.* **2009**, *63*, 245–262.
- (10) Smith, G. D.; Clark, R. J. H. *J. Archaeol. Sci.* **2004**, *31*, 1137–1160.
- (11) Allemand, C. D. *Appl. Spectrosc.* **1970**, *24*, 348–353.
- (12) Koningstein, J. A.; Bernstein, H. J. *Spectrochim. Acta* **1962**, *18*, 1249–1255.
- (13) Strommen, D. P. *J. Chem. Educ.* **1992**, *69*, 803–807.
- (14) Tuschel, D. *Spectroscopy* **2014**, *29*, 15–22.
- (15) Penna, T. C.; Faria, L. F. O.; Ribeiro, M. C. C. *J. Mol. Liq.* **2015**, *209*, 676–682.
- (16) Moschovi, A. M.; Ntais, S.; Dracopoulos, V.; Nikolakis, V. *Vib. Spectrosc.* **2012**, *63*, 350–359.
- (17) Egermann, J.; Seeger, T.; Leipertz, A. *Appl. Opt.* **2004**, *43*, 5564–5574.
- (18) Kiefer, J. *Analyst* **2015**, *140*, 5012–5018.
- (19) Kiefer, J.; Noack, K. *Analyst* **2015**, *140*, 1787–1790.
- (20) Kiefer, J.; Fries, J.; Leipertz, A. *Appl. Spectrosc.* **2007**, *61*, 1306–1311.
- (21) Warner, I. M.; Callis, J. B.; Davidson, E. R.; Christian, G. D. *Clin. Chem.* **1976**, *22*, 1483–1492.
- (22) Warner, I. M.; Callis, J. B.; Davidson, E. R.; Gouterman, M.; Christian, G. D. *Anal. Lett.* **1975**, *8*, 665–681.
- (23) Kiefer, J. *Meas. Sci. Technol.* **2017**, *28*, 067001.
- (24) Greer, J. S.; Petrov, G. L.; Yakovlev, V. V. *J. Raman Spectrosc.* **2013**, *44*, 1058–1059.
- (25) Kiefer, J. *J. Raman Spectrosc.* **2014**, *45*, 980–983.
- (26) Grüber, K.; Kiefer, J. *J. Raman Spectrosc.* **2016**, *47*, 1049–1055.
- (27) Bennett, J. M. In *Handbook of Optics*; Bass, M., Decusatis, C., Lakshminarayanan, V., Li, G., MacDonald, C., Mahajan, V., Van Stryland, E., Eds.; McGraw Hill Professional: New York, 2009.
- (28) Frosch, T.; Meyer, T.; Schmitt, M.; Popp, J. *Anal. Chem.* **2007**, *79*, 6159–6166.
- (29) Schrader, B.; VCH Verlagsgesellschaft: Weinheim, Germany, 1995.
- (30) Atamas, N. A.; Yaremko, A. M.; Bulavin, L. A.; Pogorelov, V. E.; Berski, S.; Latajka, Z.; Ratajczak, H.; Abkowicz-Bieńkoc, A. *J. Mol. Struct.* **2002**, *605*, 187–198.
- (31) Atamas, N. A.; Yaremko, A. M.; Seeger, T.; Leipertz, A.; Bienko, A.; Latajka, Z.; Ratajczak, H.; Barnes, A. J. *J. Mol. Struct.* **2004**, *708*, 189–195.
- (32) Ishiyama, T.; Sokolov, V. V.; Morita, A. *J. Chem. Phys.* **2011**, *134*, 024509.
- (33) Sceats, M. G.; Stavola, M.; Rice, S. A. *J. Chem. Phys.* **1979**, *71*, 983–990.
- (34) Skripkin, M. Y.; Lindqvist-Reis, P.; Abbasi, A.; Mink, J.; Persson, I.; Sandström, M. *Dalton Trans.* **2004**, 4038–4049.
- (35) Sastry, M. I. S.; Singh, S. *Can. J. Chem.* **1985**, *63*, 1351–1356.
- (36) Jüngst, N.; Williamson, A. P.; Kiefer, J. *Appl. Phys. B: Lasers Opt.* **2017**, *123*, 128.